PORT SAID ENGINEERING RESEARCH JOURNAL
Faculty of Engineering - Port Said University
Volume 27 No. 4 pp: 116:123

Numerical Investigation of Bottom Step Height Effect on the Hydrodynamic Performance of High-Speed Planing Crafts

M. M. Gaafary[1], M. M. Fahmy[2], M. M. Moustafa[3]*

[1]*Naval Architecture and Marine Engineering Department, Faculty of Engineering, Port Said University, Port Said, Egypt, mo2mengaafary@eng.psu.edu.eg*

[2]*Naval Architecture and Marine Engineering Department, Faculty of Engineering, Port Said University, Port Said, Egypt, m.fahmy@eng.psu.edu.eg*

[3]*Naval Architecture and Marine Engineering Department, Faculty of Engineering, Port Said University, Port Said, Egypt, moustafa3875@eng.psu.edu.eg*

**Corresponding author, DOI: 10.21608/PSERJ.2023.208843.1231*

Received 3-5-2023
Revised 25-7-2023
Accepted 10-10-2023

ABSTRACT

The utilization of transverse steps at the bottom of high-speed planning crafts represents an important geometric modification to improve their hydrodynamic performance. However, there are insufficient research investigations on the hydrodynamic effects of various step geometries on the performance of these stepped crafts. This paper aims to address this research gap by examining several types of steps and their potential impact on the hydrodynamic performance of stepped crafts. Ansys-Fluent, as a CFD software, is applied in this article, to investigate the performance of stepped planing crafts. The results are validated using both experimental and numerical data. For this study, three different step heights are considered, and a standard k–ε turbulence model is chosen. The distribution of pressure on the hull and the lift/drag ratios of high-speed stepped planing craft are determined, Additionally, a multiphase Volume of Fluid (VOF) model is employed for simulating the free-surface flow over the hull and calculations are performed over a specified speed range for each step height. The results demonstrate that the step height positively affects the hydrodynamic performance of the investigated crafts. The most appropriate step height is identified and recommended for optimal performance.

Keywords: Step Geometry; Hydrodynamic Performance; Stepped hull; Planing Crafts.

1. INTRODUCTION

Odd M. Faltinsen [1] found that high-speed planing boats operate within the range of Froude numbers that are higher than 1.2, which means that in addition to static buoyancy, the boat's weight is additionally supported by the normal to bottom dynamic pressure created by speed. The hull speed of these boat types will therefore be increased by improving their hydrodynamic performance, which can be achieved by various geometric interpretation modifications. One of the suggested modifications is the introduction of a transverse step, which reduces the boat's wetted surface area and, in turn, the drag. It also results in a uniform pressure distribution along the bottom, which enhances longitudinal stability.

Clement E. [2] was the first to experimentally investigate the patterns of drag and fluid flow in planing crafts, followed by Savitsky [3], who developed a few semi-empirical equations for the purpose of estimating both the drag and lift forces exerted on planing crafts. After a while, numerical investigations of planing crafts were carried out by Brizzolara S, Serra F. [4] and validated with previously published experiment data and semi-empirical equations of Savitsky [3] Also, Svahn D [5] developed the empirical theory of Savitsky [3] and predicted the power of a stepped hull, whereas Savitsky D, Morabito M. [6] studied the wave patterns induced by the wake of the forebody of stepped planing hulls. In addition, De Marco et al. [7] have carried out numerical and experimental investigations of stepped planing hulls.

Furthermore, Najafi A, Nowruzi H. [8] have provided a summary of the advances made in the field of step

geometry and its influence on hydrodynamic performance of stepped planing crafts.

Deadrise, step profile shape, distance from the transom, and step height are factors that might influence the hydrodynamic performance of stepped planning crafts. According to Najafi A, Nowruzi H.[8], there is a lack of research on the effects of various types of steps on the hydrodynamic characteristics of stepped planing hulls. Therefore, the main goal of this article is to extend the study to cover different stepped planing hull types.

The primary objective of this research is to narrow the research gap regarding the diverse types of bottom steps geometry and their impact on the hydrodynamic characteristics of stepped planing crafts. The study is divided into two main sections.

In the first section, our focus is on the model utilized and the available experimental and numerical data. To achieve this, we employed the D.J Taunton et al. [9] model and validated the numerical tool using experimental and numerical data from Bakhtiari M et al. [10].

The second section of the research involves introducing modifications to the model and examining their effects on the hydrodynamic performance of stepped planing crafts. We drew guidance from the modifications implemented by Najafi A, Nowruzi H. [8] and analyzed how they could potentially influence the hydrodynamic characteristics of stepped planing crafts.

By conducting this research, we aim to contribute to a better understanding of the effects of different bottom step types on the hydrodynamic performance of stepped planing craft.

2. COMPUTATION PROCESS DOMAIN & BOUNDARIES

In this study, a numerical analysis employing the CFD-Fluent simulation code is conducted, where the governing equations are stated in Appendix 1. The process includes importing the geometry of the chosen hull model, generating the domain and meshes, specifying the boundaries, defining parameters for the solver, conducting the calculations, and getting the outcomes.

Finally, the numerical results are validated by comparison with other results of two published methods. In this code, The Reynolds Average Navier-Stokes (RANS) equations with turbulent model k–ε coupled with multiphase VOF model have been solved for the turbulent free-surface flow in a specific developed mesh.

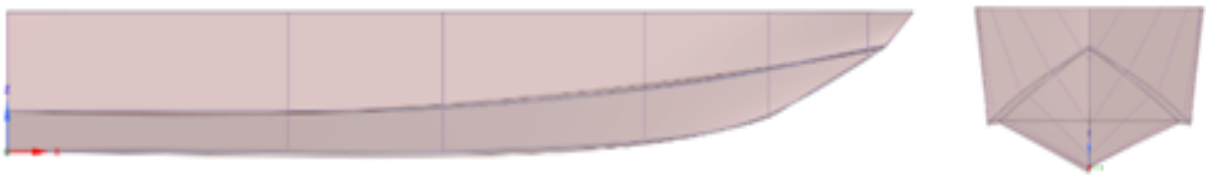

Figure 1: AutoCAD Drawing of Non-stepped planing hull

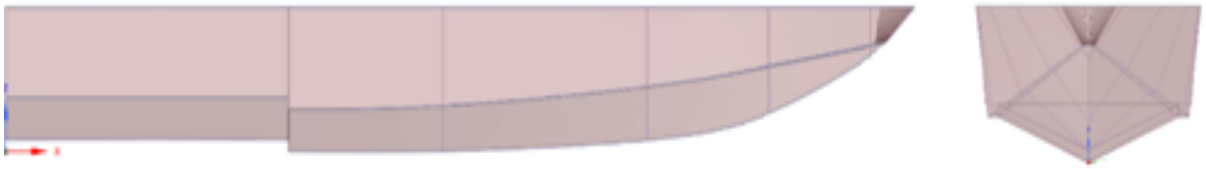

Figure 2: AutoCAD Drawing of One step planing hull

Table 1. Design Features of the Selected Model

LOA (m)	2
B (m)	0.46
T (m)	0.09
Weight (N)	243.4
Deadrise (°)	22.5
Step height (m)	0.02
Step distance measured from the transom (m)	0.62

In the computations for the current investigation, a high-speed, hard-chined, stepped hull is used. Two models are used (one with one step and the other without). At University of Southampton, these models were tested by D.J. Taunton et al. [9], and the results of their study are publicly available. The AutoCAD drawings of these models are shown in Figures 1 and 2, and Table 1 lists their design features.

Since the flow around the boat is symmetrical regarding the hull's centerline, only one side is used for the calculations. Also, the computational domain is chosen to have a size large enough to apply the proper boundary conditions and, as a result, produce more accurate solutions, see Fig. 3. It is specified that the velocity at the inlet is equal to the hull velocity. Based on the water depth at the outlet, the hydrostatic pressure can be calculated.

On the top boundary, where air can pass through it, an opening boundary condition is implemented. The symmetry condition is established for the hull's centerline plane. The hull surface is subject to a wall boundary condition, while the bottom and side boundaries are subject to free slip wall boundary conditions.

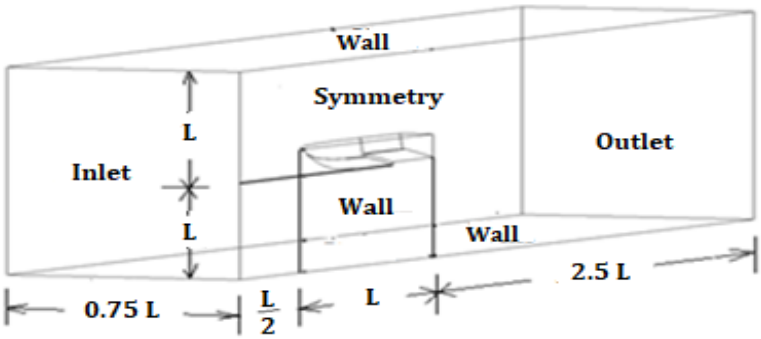

Figure 3: Computational Process Domain & Boundaries

Since geometry is considered complex, the entire solution domain is discretized using an unstructured tetrahedral mesh. A high-resolution inflating layer mesh of about 15 layers with a y+ of 40 (consistent with the underlying turbulent model) is utilized inside the boundary layer region due to the significant velocity variations in the wall-normal direction closest to the wall. The mesh quality has an important influence on the accuracy of the numerical outputs, and smaller mesh cells produce more precise values. However, doing so raises the total number of cells and, hence, the overall cost of the computation process.

Therefore, the refinement of the mesh will only be utilized in the areas where it is anticipated that the solution variables will exhibit higher gradients. To precisely capture the air-water interface, a refinement process is done to a region near the free-surface. The area closest to the hull, where separation, reattachment, and water spray occur, undergoes further refining.

The regions of refinement and the grid of computation are illustrated in Figures. 4, 5, and 6. In the same figures, in magnified views, it is easy to observe how the step's inflating layer mesh is laid out and which parts have higher precision solver setting utilized in the

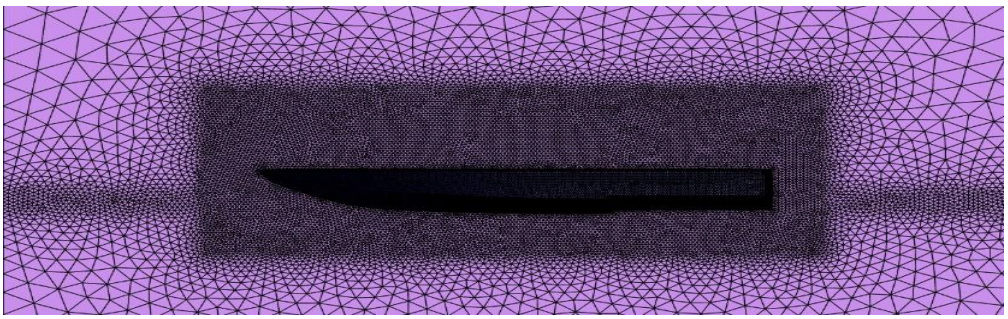

Figure 4*:* Computational grid

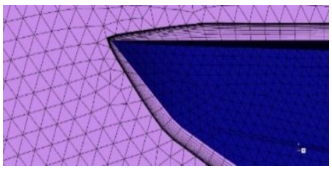

Figure 5*:* Boundary Layer at Boat's Bow

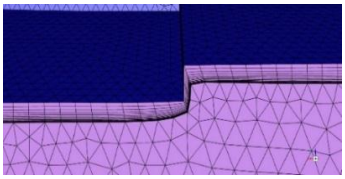

Figure 6*:* Boundary Layer at Step Location

current simulations are tabulated as shown in Table 2.

Table 2. solver settings

Item	Setting
Analysis type	Steady state
Turbulent model	Realizable k-ε
Multiphase model	Homogenous
Spatial discretization scheme	Second order upwind
Volume fraction coupling	Coupled
Convergence criteria	RMS 10E-4

3. FINDINGS & DISCUSSION

This section presents the numerical findings that were obtained for speeds ranging from 4 to 8 m/s, with an interval of 2 m/s. In accordance with experimental findings by D.J. Taunton et al. [9], varied draughts and trims have been taken into consideration at each speed. For validating the findings of the present approach, both stepped and non-stepped hulls' experimental and numerical data from Veysi STG et al.'s [11] work are compared against the results of numerical calculations, see Figure 7.

Working fluid of water has a density (ρ) of 997 kg/m^3, viscosity (μ) of 8.889×10^{-4} kg/$m.s$, and air has ρ = 1.185 kg/m^3 and μ = 1.83×10^{-5} kg/$m.s$. Iterations proceed until the remaining errors go below 10^{-4} and the total drag approaches a steady state to be sure that the result in each computation converges. It should be mentioned that the step would result in a substantial reduction in the boat's overall drag. For all Froude numbers, as can be seen in Figure 7, we have the results from the current method, which exhibit satisfactory agreement with the experimental results with a reasonable average difference of about 10%.

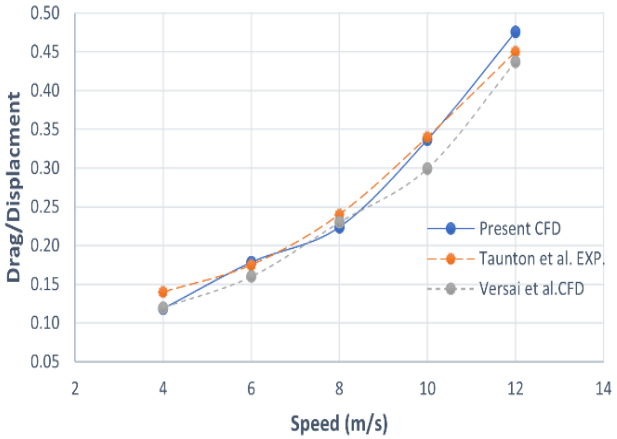

Figure 7.a: Non-stepped Hull

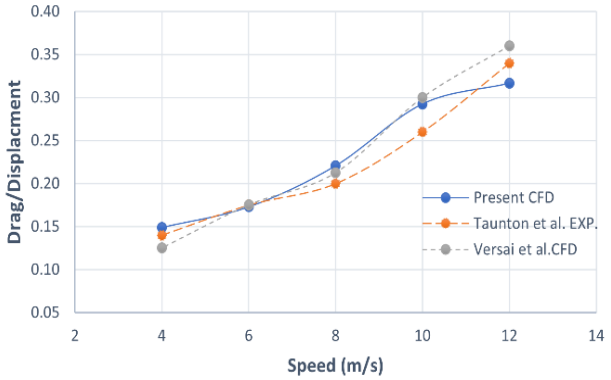

Figure 7.b: Stepped Hull

Figure 7: Validation of Present Numerical Drag Ratio with both Experimental and Numerical Methods.

Surely, the step's application positively influences the hydrodynamic performance of the stepped planning hull. The point of interest is how the step height may affect the hydrodynamic performance (Lift/Drag Ratio) at different speeds of a selected range of (4 to 8 m/s). From Figure 8, increasing the step height does not have that large or dramatic effect on the drag ratio. On the other hand, the lift ratio drops dramatically, at step height of 20 mm (about 0.79 in) then increases again.

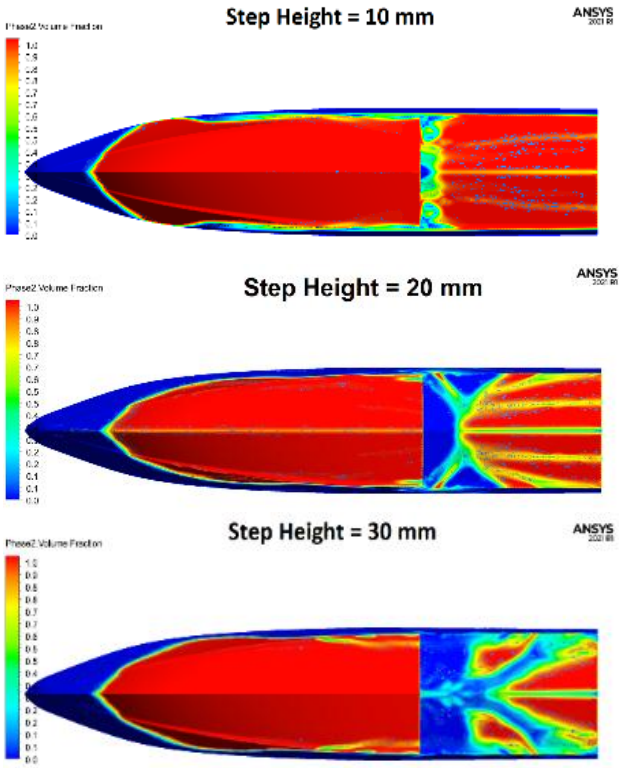

Figure 8: Effect of Step Height Increases at V = 4 m/s.

In Figure 9, at V = 6 m/s, starting from a step height of 10 mm (about 0.39 in) the lift and drag ratio behaves slightly the same way by increasing in a small value then reduces at step height of 30 mm (about 1.18 in).

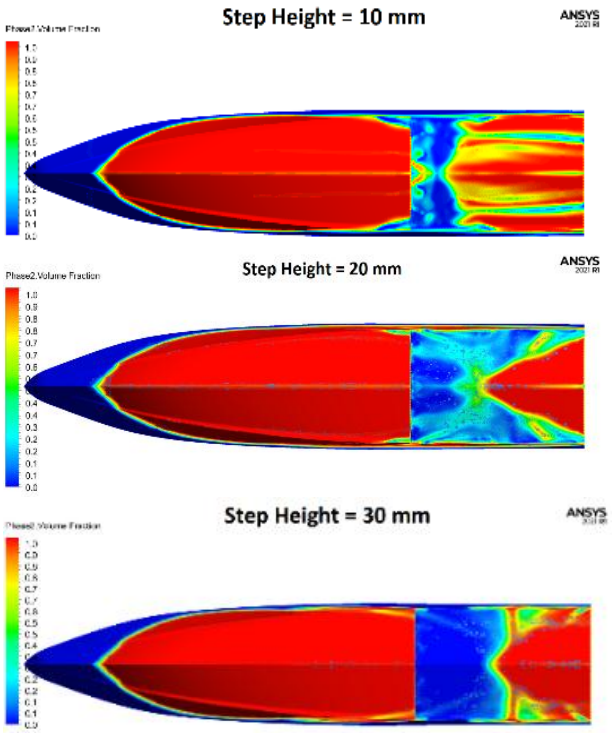

Figure 9: Effect of Step Height at V = 6 m/s

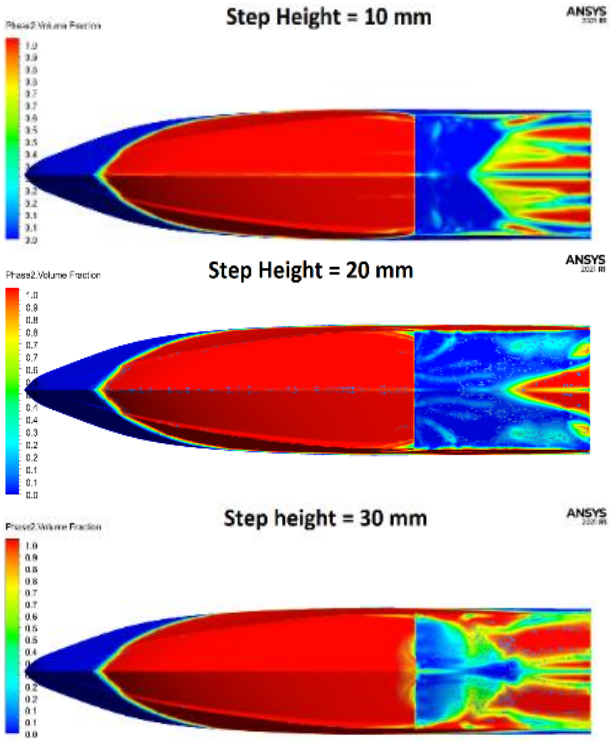

Figure 10: Effect of Step Height at V = 8 m/s

In Figure 10, from the first point, lift has decreased and stayed at a steady value until it reaches the last point. While the drag ratio increases until it reaches its peak at a step height of 20 mm (about 0.79 in) then decreases to the end. Hence, it can be concluded that the step height of 20 mm (about 0.79 in) shows the optimum performance of both lift and drag ratio compared with the other two heights, see Figure 11.

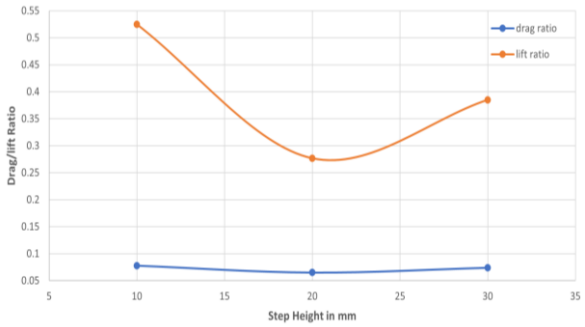

Figure 11.a: Drag/Lift Ratios at V = 4 m/s.

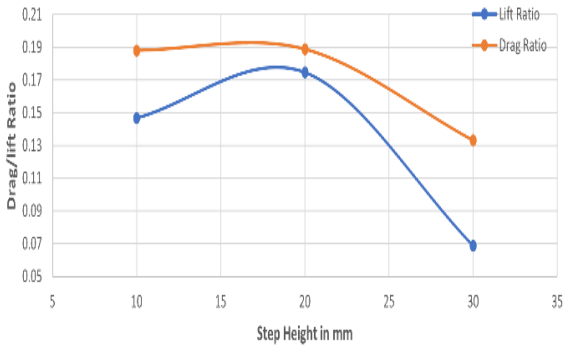

Figure 11.b Drag/Lift Ratios at V = 6 m/s

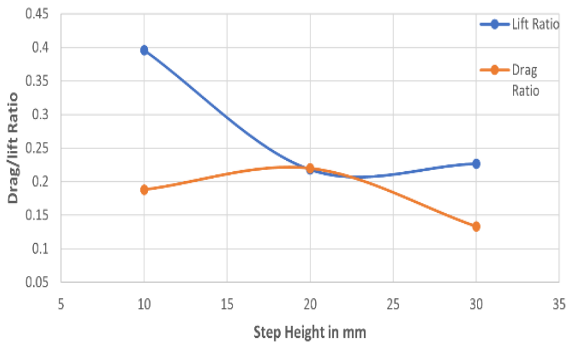

Figure 11.c: Drag/Lift Ratios at V = 8 m/s

Figure 11: Drag and Lift Ratios at Different Speed and Step Heights

In a deeper look, pressure distribution may explain the interaction of water and boat surface, and its variance with step height increase. Figures 12, 13, and 14 depict the distribution of pressure on the hull's bottom at step heights of 10mm, 20 mm, and 30 mm, respectively.

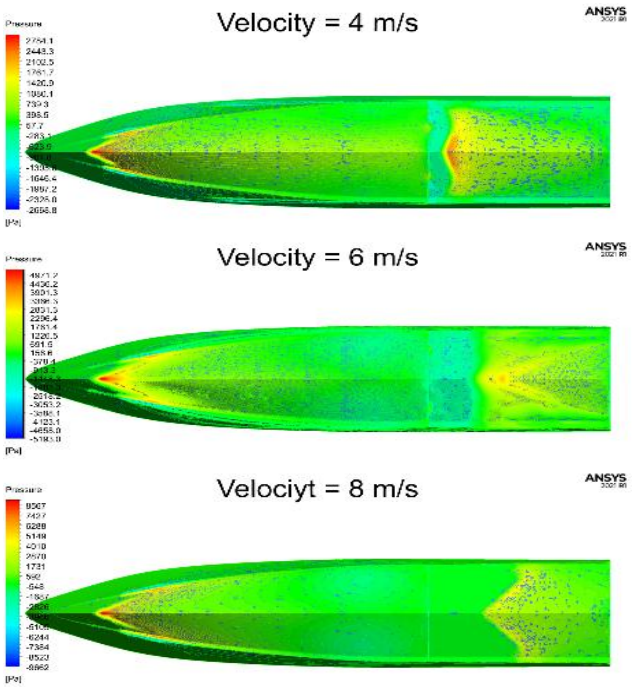

Figure 12: Pressure Distribution at a Step Height of 10 mm (about 0.39 in)

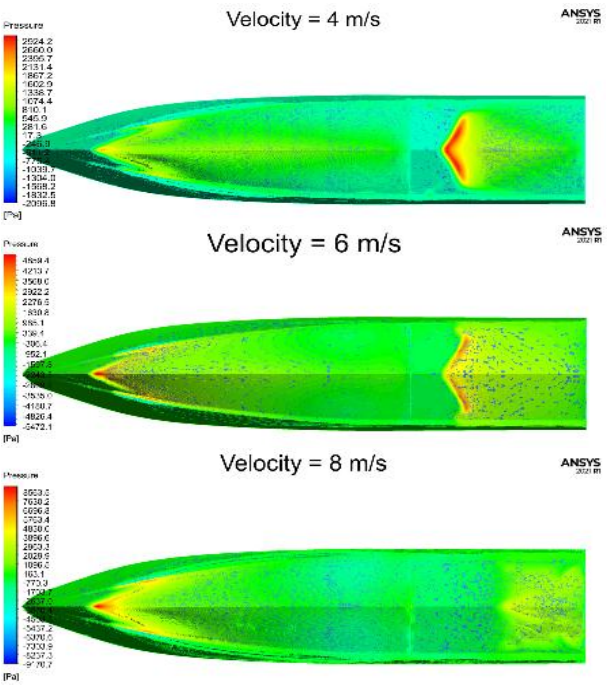

Figure 13: Pressure Distribution at a Step Height of 20 mm (about 0.79 in)

In Fiure.12 one may notice that there are two pressure points, one in the fore body and the other is located after the step and differ according to the speed and the step height. At step height of 10 mm (about 0.39 in), the last pressure point travels far as the speed growth also the pressure reduces gradually, by increasing the step with an interval of 10 mm (about 0.39 in). Whereas in Figure 13, the pressure intensity appears to decrease as the speed increases and reaches a further point compared to that of a step height of 10 mm (about 0.39 in). Of the three step heights, one may notice that the hull's bottom experiences the lowest pressure at step heights of 30 mm (about 1.18 in), notably at speeds of 8 m/s, while at 6 m/s, the pressure is localized around the second pressure point (see Figure 14). To conclude a comment on the pressure distribution, one might say that the speed growth affects the position of the second pressure point and increases the step height positively affects the pressure distribution around the bottom of the planing boat.

4. CONCLUSIONS

The effect of planing hull bottom step on the hydrodynamic characteristics of a typical high-speed hard-chined planing hull model is investigated. Using a numerical technique at a speed range from 4 to 8 m/s with intervals of about 2 m/s. To simulate the free-surface flow around a high-speed planing hull, the turbulent model k-ε coupled with the multiphase VOF model is employed.

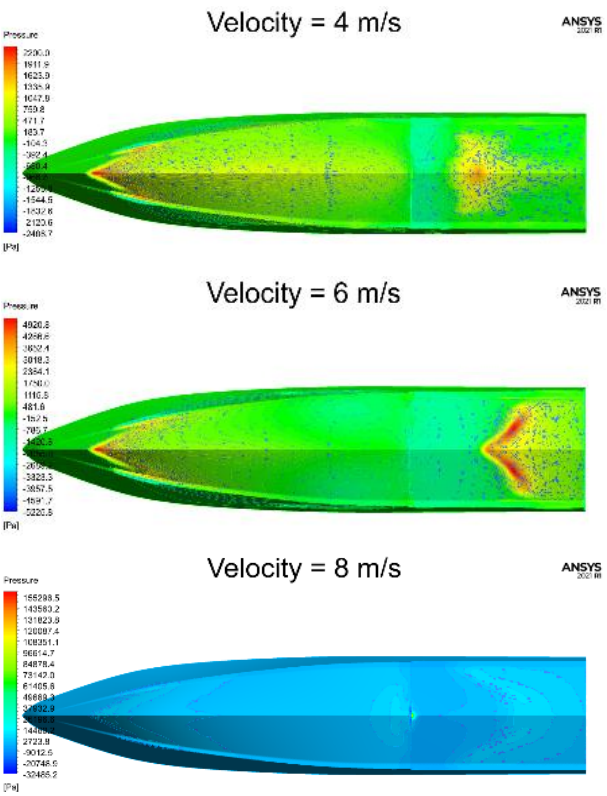

Figure 14: pressure distribution at a step height of 30 mm (about 0.79 in)

Both planing hulls with steps and those without steps can be accurately simulated by these models. For a precise drag calculation, the CFD code utilized in the current investigation can be applied. Hence, the results of the present developed numerical method are checked against previously published experimental and numerical data and found to be in good agreement (with an average error of 10%). The pressure distribution resulted from these CFD codes also showed a good consistency. Numerical results for different step heights (10, 20 and 30 mm) show that the best lift/drag ratio occurs at step height of 20 mm (about 0.79 in) which is the optimum choice.

Finally, there is a future plan to include more variables in the optimum design of a stepped planing hull as well as to employ a neural network to produce the step geometry.

Contribution Statement

M. M. Gaafary: Conceptualization, Methodology, writing review & editing, Supervision. **M. M. Fahmy:** Conceptualization, Methodology, writing original draft. **M. M. Moustafa:** Conceptualization, Methodology, Writing review & editing, Supervision.

Declaration of Competing Interest

The authors claim to be unaware of any financial or personal disputes that might have any effect on the work reported in this article.

APPENDIX 1: GOVERNING EQUATIONS

The governing equations of continuity and RANS can be applied for simulating the fluid flow over a planing hull as follows:

$$\frac{\partial \rho}{\partial t} + \frac{\partial}{\partial x_j}(\rho u_j) = 0 \quad (1)$$

$$\frac{\partial \rho u_j}{\partial t} + \frac{\partial}{\partial x_j}(\rho u_i u_j) = -\frac{\partial P}{\partial x_i} + \frac{\partial}{x_j}(\tau_{ij} - \rho\overline{u_i{}' u_j{}'}) + g_i, \quad (2)$$

Where the terms for velocity, pressure, and gravitational acceleration are u, P, and g, respectively. While the Reynolds stresses are represented by the term $-\rho\overline{u_i{}' u_j{}'}$. In accordance with the hypothesis of eddy viscosity, mean velocity gradients and eddy viscosity are linked to Reynolds stresses. The Reynolds averaged momentum formula changes because of this hypothesis to:

$$\frac{\partial \rho u_i}{\partial t} + \frac{\partial}{\partial x_j}(\rho u_i u_j) = -\frac{\partial P}{\partial x_i} + \frac{\partial}{x_j}\left[\mu_{eff}\left(\frac{\partial \rho u_i}{\partial x_j} + \frac{\partial \rho u_j}{\partial x_i}\right)\right] + g_i, \quad (3)$$

In this case, μ_{eff} is the effective viscosity as determined by:

$$\mu_{eff} = \mu + \mu_t. \quad (4)$$

Turbulent model

For simulating the turbulence in the flow in this investigation, the standard two equations k-ε have been applied. The k-ε model considers the following relationship between the viscosity of the turbulence and its kinetic energy (k) and dissipation rate (ε):

$$\mu_t = c_\mu \rho \frac{k^2}{\varepsilon}, \quad (5)$$

Where, k and ε are determined using the following transport equations and c_μ is a constant.

$$\frac{\partial(\rho k)}{\partial t} + \frac{\partial}{\partial x_j}(\rho u_j k) = \frac{\partial}{\partial x_j}\left[\left(\mu + \frac{\mu_t}{\sigma_k}\right)\frac{\partial k}{\partial x_j}\right] + p_k - \rho\varepsilon, \quad (6)$$

$$\frac{\partial(\rho \varepsilon)}{\partial t} + \frac{\partial}{\partial x_j}(\rho u_j \varepsilon) = \frac{\partial}{\partial x_j}\left[\left(\mu + \frac{\mu_t}{\sigma_\varepsilon}\right)\frac{\partial \varepsilon}{\partial x_j}\right] + \frac{\varepsilon}{k}(c_{\varepsilon 1} p_k - c_{\varepsilon 2}\rho\varepsilon) \quad (7)$$

Where, $c_{\varepsilon 1}$, $c_{\varepsilon 2}$, σ_k , and σ_ε are constants. *pk* is the parameter responsible for producing turbulence due to viscous forces.

Multiphase model

A VOF model has been employed for capturing the air-water interface; in this instance, the volume ratio of the two phases is calculated using the following transport equation:

$$\frac{\partial \alpha}{\partial t} + \vec{\nabla}.(\propto \vec{u}) = 0 \quad (8)$$

The volume fraction of each phase inside of each computational cell is represented by $0 < \propto < 1$. Where,

$$\sum_{k=1}^{2} \propto_k = 1 \quad (9)$$

The Navier-Stokes and continuity equations can be solved by the volume of fluid technique to produce an effective fluid having the following effective properties within every cell:

$$\rho_{eff} = \propto.\rho_1 + (1-\propto).\rho_2 \quad (10)$$

$$v_{eff} = \propto.v_1 + (1-\propto).v_2. \quad (11)$$

Hence, the computational cell lies within fluid one if α = 0 and fluid two if α = 1. However, if $0 < \propto < 1$ the cell will be on the free surface.

5. REFERENCES

[1] Odd M. Faltinsen. Hydrodynamics of High-Speed Marine Vehicles. vol. 66. 2012.

[2] Clement E. C. Trans Sname 1963;64:1956.

[3] Savitsky. Savitsky_64_Hydroynamic design of planing hulls.pdf 1964.

[4] Brizzolara S, Serra F. Accuracy of CFD codes in the prediction of planing surfaces hydrodyamic characteristics. 2nd Int Conf Mar Res Transp 2007:147–58.

[5] Svahn D. Performance Prediction of Hulls with Transverse Steps 2009.

[6] Savitsky D, Morabito M. Surface wave contours associated with the forebody wake of stepped planing hulls. Mar Technol 2010;47:1–16. https://doi.org/10.5957/mtsn.2010.47.1.1.

[7] De Marco A, Mancini S, Miranda S, Scognamiglio R, Vitiello L. Experimental and

numerical hydrodynamic analysis of a stepped planing hull. Appl Ocean Res 2017;64:135–54. https://doi.org/10.1016/j.apor.2017.02.004.

[8] Najafi A, Nowruzi H. On hydrodynamic analysis of stepped planing crafts. J Ocean Eng Sci 2019;4:238–51. https://doi.org/10.1016/j.joes.2019.04.007.

[9] D.J. Taunton et al. Characteristics of a series of high speed hard chine planing hulls – Part 1: Performance in calm water. Int J Small Cr Technol · January 20 2010.

https://doi.org/10.3940/rina.ijsct.2010.b2.96.

[10] Veysi STG, Bakhtiari M, Ghassemi H, Ghiasi M. Toward numerical modeling of the stepped and non‐stepped planing hull. J Brazilian Soc Mech Sci Eng 2015;37:1635–45.

https://doi.org/10.1007/s40430-014-0266-4.